

Published in final edited form as:

Cardiovasc Pathol. 2011 November ; 20(6): 334–342. doi:10.1016/j.carpath.2010.10.002.

Differential Proteoglycan and Hyaluronan Distribution in Calcified Aortic Valves

Elizabeth H. Stephens, PhD¹, Jerome G. Saltarrelli, PhD¹, L. Scott Baggett, PhD¹, Indrajit Nandi, BS¹, Joyce J. Kuo, BS¹, Alan R. Davis, PhD², Elizabeth A. Olmstead-Davis, PhD², Michael J. Reardon, MD⁴, Joel D. Morrisett, PhD³, and K. Jane Grande-Allen, PhD¹

¹Department of Bioengineering, Rice University, Houston, TX 77005

²Center for Cell and Gene Therapy, Baylor College of Medicine, Houston, TX, 77030

³Departments of Medicine and Biochemistry, Baylor College of Medicine, Houston, TX

⁴Department of Cardiovascular Surgery, The Methodist Hospital, Houston, TX 77030

Abstract

Background—While the prevalence of calcified aortic valve disease continues to rise and no pharmacological treatments exist, little is known regarding the pathogenesis of the disease. Proteoglycans and the glycosaminoglycan hyaluronan are involved in calcification in arteriosclerosis and their characterization in calcified aortic valves may lend insight into the pathogenesis of the disease.

Methods—14 calcified aortic valves removed during valve replacement surgery were immunohistochemically stained for the proteoglycans (PGs) decorin, biglycan, and versican, as well as the glycosaminoglycan hyaluronan. Staining intensity was evaluated in the following regions of interest: center of calcified nodule, edge of nodule, tissue directly surrounding nodule; center and tissue surrounding small “prenodules”; and fibrosa layer of normal regions of the leaflet distanced from the nodule.

Results—Decorin, biglycan, and versican, as well as hyaluronan, were abundantly present immediately surrounding the calcified nodules, but minimally within the nodule itself. Expression of decorin and biglycan in and surrounding prenodules was greater than in the edge and center regions of mature nodules. The levels of expression of the PGs and hyaluronan were highly correlated with one another in the different regions of the valve.

Conclusions—The three PGs and hyaluronan demonstrated distinctive localization relative to nodules within calcified aortic valves, where they likely mediate lipid retention, cell proliferation, and extracellular matrix remodeling, and motivate further study. Comparisons between expression of these components in mature nodules and prenodules suggest distinct roles for these components in nodule progression, especially in the tissues surrounding the nodules.

Keywords

proteoglycans; hyaluronan; calcification; aortic valve; immunohistochemistry

© 2010 Elsevier Inc. All rights reserved.

Address for correspondence: K. Jane Grande-Allen, Ph.D., Department of Bioengineering, Rice University, 6100 Main St., MS 142, Houston, TX 77005, Phone: 713-348-3704, Fax: 713-348-5877, grande@rice.edu.

Publisher's Disclaimer: This is a PDF file of an unedited manuscript that has been accepted for publication. As a service to our customers we are providing this early version of the manuscript. The manuscript will undergo copyediting, typesetting, and review of the resulting proof before it is published in its final citable form. Please note that during the production process errors may be discovered which could affect the content, and all legal disclaimers that apply to the journal pertain.

INTRODUCTION

The prevalence of calcific aortic valve disease (CAVD) is rising and represents the second most common indication for cardiac surgery in elderly patients [1]. CAVD is associated with aging [1], male gender [2], and metabolic syndrome [3], and is only treatable by surgical replacement of the stenotic valve with a mechanical, bioprosthetic or biological valve [4]. CAVD is marked by lipid retention and monocyte infiltration in its early sclerotic stage, resulting in leaflet thickening, whereas the later stenotic stage is characterized by thickened, stiff, calcified leaflets containing heterotopic bone [5]. At the present time, there are no pharmacological therapies designed expressly for the treatment of CAVD, largely due to our limited understanding of the disease mechanisms. Statins initially appeared promising as a means of preventing or reversing CAVD in patients, based on the ability of these lipid-lowering drugs to reduce valve calcification *in vitro* [6,7] and in animal models [8–10], but unfortunately that promise has not translated to a significant improvement in prospective clinical trials [11–13]. Thus, investigators are examining calcified heart valve lesions and valve cells to determine the roles of osteogenic and inflammation-related genes, various extracellular matrix components, matrix remodeling enzymes, lipids, oxidative stress, and mechanical stress [10,14–17].

A potential role of the extracellular matrix in the initiation and progression of CAVD is suggested by early valve lesions specifically developing within the unique extracellular matrix composition of the fibrosa layer within the leaflet. This layer contains highly aligned collagen as well as the proteoglycans (PGs) decorin and biglycan [18,19]. A PG consists of a core protein covalently linked to at least one glycosaminoglycan (GAG) chain; with the exception of hyaluronan (HA), all GAGs exist *in vivo* as components of PGs. The small leucine-rich PGs decorin and biglycan are themselves interesting because these PGs mediate collagen fibrillogenesis [20] and sequester transforming growth factor-beta (TGF- β) [21], and their GAG chains are well known to bind to lipids and lipoproteins in the progression of atherosclerosis [22]. HA also demonstrates the ability to retain lipids [23,24]. In atherosclerosis, lipid retention and oxidation triggers inflammation, the proliferation and transdifferentiation of smooth muscle cells (SMCs), angiotensin receptor activation, and free radical formation, among other processes [15,22,25,26]; similar mechanisms may occur in aortic valve sclerosis. Intriguingly, O'Brien et al. suggested that biglycan and decorin are co-localized with apolipoproteins in these lipid-rich valve lesions [27], but this notion was never fully explored. The ability of HA to attract and promote the accumulation of monocytes in atherosclerosis [28] suggests an additional potential role for these GAGs in the chronic inflammation of valve disease. Finally, HA has also been shown to be an effective medium for the delivery of bone morphogenic protein (BMP)-2 [29,30], which mediates both normal bony ossification and abnormal heterotopic ossification in many tissues including heart valves [15]. The PGs decorin, biglycan, and versican, as well as all four classes of GAGs, are found in varying abundance in heart valves [19,31,32], and have been studied in bioprosthetic aortic valves [33] and myxomatous mitral valves [34], but have received little attention regarding CAVD. It is also known that mechanical stimulation of valvular interstitial cells regulates their production of extracellular matrix [35], including PGs [36]. Since the distribution of mechanical loading across calcified aortic valves is abnormal, and may feature stress concentrations surrounding calcific nodules, these conditions may promote alterations in the normal patterns of PG composition.

Therefore, the purpose of this study was to assess the location and abundance of specific PGs and the GAG HA relative to calcific nodules in diseased aortic valves. Such characterization could improve our understanding of this common valve disease and contribute towards developing novel treatments.

METHODS

Tissue Procurement and Decalcification

Calcified aortic valves were removed during valve replacement surgery and did not show signs of rheumatic disease (as diagnosed by the attending surgeons and pathologists). These tissues were obtained from the Methodist DeBakey Heart and Vascular Center of the Methodist Hospital (Houston, TX) and the Cooperative Human Tissue Network (CHTN) (n=14, mean age 65±15, 80% male). At Methodist, patients with aortic insufficiency were considered eligible for aortic valve replacement if they had ejection fractions < 55% and an end-systolic left ventricular diameter > 55 mm. Patients with aortic stenosis were eligible for aortic valve replacement only if they were symptomatic and demonstrated any of the following characteristics: aortic valve area < 1.0 cm² or < 0.6 cm²/m² (normalized to body surface area); echocardiographic flow velocity > 4 m/sec², or transvalvular gradient > 50 mmHg. Comparable inclusion criteria were employed for valves obtained through CHTN. Study authors KJGA and JDM obtained approval from the Institutional Review Boards at Rice University and Baylor College of Medicine for the research use of these tissues. The calcified aortic valves obtained from Methodist were selected at random from a group of surgical specimens collected for analysis by study author JDM. The only defining characteristic of the selected valves was having at least one intact leaflet, as opposed to having been surgically resected only as calcified leaflet fragments. These valves were either stored in 50% glycerol in phosphate-buffered saline (PBS) at -20°C or in RNAlater (Applied Biosystems, Foster City, CA) at -80°C. Prior to histological processing, glycerol or RNAlater was removed by dialyzing overnight in fresh PBS. Afterwards, several 2–3 millimeter radial strips were cut from each leaflet and placed into 10% formic acid at room temperature for 12–24 hours (depending on level of calcification) to decalcify the sections allowing routine paraffin embedding; it has been previously shown that formic acid treatment decalcifies tissues without damaging antigenicity [37,38] or PG content [39,40]. After a palpable level of decalcification was achieved, diseased valves were embedded in paraffin and sectioned according to routine procedures. The 4 specimens obtained from the CHTN were already decalcified and embedded in paraffin and were similarly sectioned. The exact method of decalcification for the CHTN samples is undetermined; however, the CHTN stained tissues could not be distinguished from samples from Methodist.

Histology and Immunohistochemistry

Sections were stained with Movat pentachrome to demonstrate the heterogeneous microstructure of the leaflet. Immunohistochemistry (IHC) was performed to localize the PGs decorin, biglycan and versican within the valve tissues using antibodies against their respective core proteins. Briefly, tissue slides were processed through a series of graded alcohols and hydrated to water. All slides were pretreated with chondroitinase ABC (200 mU/ml, 37°C, 1 hour) to remove the GAG chains from the PG core proteins. Sections were blocked with 10% goat-serum (Sigma, St. Louis, MO), then incubated with primary antibodies against PGs overnight at 4°C. The rabbit anti-human decorin (LF-136, dilution 1:800) and biglycan antibodies (LF-51, dilution 1:2000) were generously provided by Larry Fisher, Ph.D., NIH [41]; the murine antibody against mammalian versican (clone 2-B-1, dilution 1:5000) was purchased from Associates of Cape Cod (East Falmouth, MA). After rinsing in PBS, biotinylated secondary antibodies were applied (goat anti-mouse or anti-rabbit IgG, Jackson Immunoresearch Inc., West Grove, PA) for 1 hour at room temperature. Positive staining was demonstrated by a chromogen reaction using Vectastain Elite ABC and diaminobenzidine kits (Vector, Burlingame, CA). The presence of HA was demonstrated by histochemical binding to an HA binding protein (HABP), which contains the “link” domain protein that normally binds HA to aggrecan in the formation of an aggrecan aggregate. This HA staining procedure required blocking with 2% fetal bovine

serum, treating with biotinylated HABP (as described by Lara et al. [42]), then performing chromogenic detection. All samples were counterstained with hematoxylin. To minimize variability, multiple samples were taken from a given patient's valve. Negative controls for all markers were performed in the absence of the primary antibody or HABP.

Analysis of Immunohistochemical Staining

Several regions of the radially oriented leaflet sections stained for PGs and HA were evaluated to quantify the mean 8-bit intensity of brown staining using ImageJ software (NIH, Bethesda, MD). To determine the reproducibility of these mean intensity measurements, several regions were measured on two separate occasions; it was calculated that on average, the two measurements differed by approximately 7%. Because the binding of lipids by GAGs and PG is speculated to be an early event in the progression of CAVD [43], calcified nodules were categorized as large and presumably mature ("nodule") or small and presumably early-stage ("prenodule"). Prenodules were identified as substantially smaller nodules (typically $\leq 1/2$ of leaflet height), which were not continuous with the main nodule; prenodules were generally located closer to the annulus than was the main nodule (Figure 1). Regions of interest were identified in the nodule center (innermost 2/3), edge (outermost 1/3), and surrounding tissue; in the prenodule center and surrounding tissue; and in the fibrosa layer of a normal-appearing region of the same leaflet far away from the nodules.

Statistical Analysis

Statistical analysis of data was performed using SAS (Cary, NC). A multifactorial analysis of variance (ANOVA) test was used with the level of significance set at 0.05. Multiple comparisons of group means were performed using the Tukey-Kramer method for controlling maximum experimentwise error rate. Correlations between staining intensities of different proteins within individual leaflet regions (to assess protein co-localization) were calculated using Pearson Product Moments. For correlations between intensities of different matrix components, the level of significance was reduced to 0.0125 to account for 4 markers being considered.

RESULTS

As expected from numerous previous pathological descriptions [4,5,25,44], the Movat pentachrome staining showed that the diseased aortic valves contained large calcific nodules, often occupying approximately 1/3 of the radial length. The calcifications were stained dark purple by the Voerhoff's hematoxylin component of the Movat stain, making it straightforward to localize the nodule boundaries and thus identify nodule center, edge, and surrounding tissue. All 14 diseased valves had mature nodules, whereas only 7 of the valves had prenodules (Figure 1). Most valve leaflets had regions away from the nodules with a normal appearing layered structure in which the collagenous fibrosa (stained yellow by the saffron component of the Movat stain) could be identified (see asterisk in Figure 1).

The proteoglycans and HA demonstrated greatest expression in the valve tissue immediately surrounding the mature nodules (Figure 2; overall ANOVA $p < 0.0001$ for decorin, biglycan, and versican; $p = 0.0104$ for HA). There was often a distinct border of expression ending at the nodule, although in some valves there was some degree of PG and HA expression within the nodule as well. Versican and HA expression in the tissue immediately surrounding the nodule was significantly greater than in the nodule edge and prenodule (Figures 1–3). Versican expression surrounding the nodule was also greater than in the nodule center and in the normal fibrosa; versican expression in the nodule center and edge was lower than in the distal normal fibrosa. While strong versican expression often directly abutted the nodule,

HA expression often tapered off, being externally high and then decreasing approaching the edge of the nodule. Expression of biglycan within the center and edge of the nodule was significantly lower than in the tissue surrounding the nodule, in the prenodule, and in the distal normal fibrosa (Figures 3–4). Expression of decorin showed a similar regional pattern with expression being significantly lowest in the nodule edge and center. The expression of decorin and biglycan within and surrounding prenules was also greater than in the edge and center regions of mature nodules.

The levels of expression of the different PGs and HA were highly correlated with each other in different regions of the diseased aortic valves. In the tissue immediately surrounding the nodule, biglycan expression was positively correlated with expression of versican ($r=0.80$, $p=0.0003$) and HA ($r=0.71$, $p<0.002$). HA and versican were also correlated in this same region ($r=0.79$, $p=0.004$). Decorin and biglycan were positively correlated in the edge (outermost 1/3) of the nodule ($r=0.64$, $p<0.008$), and even more strongly correlated in the tissue surrounding the pre-nodule ($r=0.98$, $p=0.0005$). Interestingly, in the pre-nodule, biglycan was negatively correlated with HA ($r=-0.95$, $p<0.004$). No other significant correlations were found between the various PGs or HA in the center (inner 2/3) of the nodule nor in the distal fibrosa.

DISCUSSION

In this study, we showed that the PGs versican, decorin, and biglycan, as well as the GAG HA, are richly present within the tissue immediately surrounding the calcified nodules, but generally absent from the nodules. We also found that versican and HA are strongly abundant in the vicinity of the larger nodules, but less so in the smaller “prenodules.” These differences in the distribution of small leucine-rich PGs and the large, hydrated PG and GAG suggest that distinctive remodeling processes are occurring throughout the diseased leaflets.

The small leucine-rich PGs decorin and biglycan were abundant throughout the calcified aortic valve leaflets; based on other studies of PGs in normal and diseased cardiovascular tissues we speculate that they were likely involved with active pathological remodeling in the tissue surrounding the nodules. In normal human aortic valves, decorin and biglycan are ubiquitously distributed [18], yet frequently co-localized with collagen, which would support their role in collagen fibrillogenesis [21]. The core proteins of these small PGs are also able to bind to growth factors such as TGF- β and epidermal growth factor (EGF), and thus could influence cell proliferation. In addition, the chondroitin sulfate GAG chains on these PGs are known to bind to lipids and retain them within the local region of the calcific nodule, thereby facilitating the ability of oxidized lipids to initiate further pathological remodeling [45]. The ability of these GAG chains to bind lipids is influenced by their fine structure, meaning their chain length, the extent and pattern of sulfation, and the isoform of the uronic acid moiety [45,46]. As we could not determine by immunohistochemical detection of the PG core proteins whether or not there were differences in the fine structure of the GAG chain, it will be important to examine these small PGs and their GAG chains in the future to discern if the GAG chains in the tissue surrounding the nodule show enhanced lipid binding properties.

The novel finding of the PG versican and HA in the tissue surrounding the calcific nodule further underscores the active remodeling occurring with this area. Versican is a very large PG that contains a multidomain core protein from which emanates 15–20 very long chondroitin sulfate GAG chains. The G1 domain of the versican core protein is known to destabilize adhesive contacts [47] and has another region that promotes binding to HA to create a versican aggregate [48]. The G3 domain is also multifunctional, and contains an

EGF-like region that promotes cell proliferation [49]. The GAG chains attached to the center of the core protein imbue the PG with substantial hydration. As a result, the overall versican PG has considerable capability to swell tissues and influence regional cell proliferation and migration. Normally, versican is primarily located within the central spongiosa layer of aortic valves [18,19], where it is believed to aid in the tissue's resistance to cyclic compression and where it can provide lubrication to the outer fibrosa and ventricular layers. Similarly to decorin and especially biglycan, the GAG chains on versican could also bind lipids, as is demonstrated in atherosclerosis [50]. Versican is linked with numerous additional pathological processes in atherosclerosis as well, including interactions with inflammatory cells and cytokines, roles in platelet aggregation, interference (specific and nonspecific) with normal extracellular matrix assembly, and upregulating cell proliferation [50]. Recently, it was found that the genes for versican, biglycan, and several enzymes involved in GAG chain assembly (such as xylosyltransferase-I, β -1,4-N-acetylgalactosaminyltransferase) were upregulated in mesenchymal stem cells cultured in osteogenic medium, and that the expression of these genes was strongly and temporally associated with expression of alkaline phosphatase and osteopontin as well as von Kossa staining for mineralization [51]. Taken together, there is growing evidence pointing towards active roles of these PGs in the progression of CAVD. In addition, the tissue surrounding the calcified nodule is likely experiencing a unique mechanical stress environment that may be driving this remodeling. In the future, it will be important to investigate the influence of mechanical stimulation on aortic valvular interstitial cells' production of various PGs and how those PGs then mediate events related to heterotopic ossification.

The well recognized abilities of HA to influence cell and tissue behavior are also likely to play roles in the tissue surrounding the calcific nodules. HA is normally a linear chain of thousands of repeating, unmodified disaccharide units and can account for up to 50%–60% of all valve GAGs [31,33,34] and is secreted by valvular interstitial cells (VICs) [52,53]. In normal valves, HA is attributed with many of the same biophysical characteristics as is versican, namely promoting hydration, lubrication, and resistance to compression [19]. However, HA is abundant in atherosclerotic lesions [54], and based on selected other similarities between atherosclerosis and CAVD it is compelling to consider what factors influence HA regulation in atherosclerosis. Atherosclerotic lesions stain strongly for TGF- β , as well as for platelet-derived growth factor-AB [54] and both have been shown to regulate HA synthesis (as well as PG synthesis and GAG chain fine structure [55]) by numerous cell types [56]. VICs treated with TGF- β also upregulate HA secretion [53]. HA has been implicated in tissue responses to injury including monocyte adhesion and activation and the proliferation and migration of vascular SMCs and leukocytes [54,57]. Proliferating vascular SMCs and fibroblasts synthesize more HA [57], often as cables that bind monocytes [58]. HA also demonstrates the ability to retain lipids [23,24], leading to the development of sclerotic lesions.

Other potential therapeutic targets for atherosclerosis, and potentially for CAVD, include the three HA synthases (HAS-1, HAS-2, and HAS-3) and the HA receptors on the cell surface, namely CD44, RHAMM (the receptor for hyaluronic acid mediated motility), and HARE (HA receptor for endocytosis). It is known that in general, HA ligation to CD44 mediates leukocyte, monocyte, and macrophage recruitment, the production of several inflammatory mediators, vascular cell activation [23,58], tyrosine kinase activity of p185^{HER-2} and src and the activation of Rho and Rac-1. CD44-null mice crossed with apolipoprotein-E (apo-E) null mice had less atherosclerosis than the uncrossed apo-E null mice, despite equivalent cholesterol levels [23]. Binding of HA to RHAMM activates downstream signaling via src and Ras [58]. *In vitro*, the addition of low molecular weight HA caused a CD44-dependent upregulation of SMC proliferation (an effect also reported in VICs [59]) and VCAM-1 synthesis [23]; other HA receptors may also be involved in early lesion development [23]. *In*

vivo, these HA fragments would be generated by hyaluronidases such as Hyal-1 and Hyal-2 [60]. Taken together, the various factors that promote the formation of an HA-rich matrix likely regulate sclerotic lesion development and inflammatory responses in heart valves as well as vessels, although the roles of HA receptors, synthases, and degrading enzymes in CAVD are presently unknown.

The differences in abundance and correlations between the small PGs and the larger, hydrated versican and HA across the diseased leaflets suggests distinctive remodeling mechanisms. Each of the PGs and HA were more abundant surrounding the nodules compared to the nodule interior, suggesting that these molecules are not involved in mineralization. Decorin and biglycan, in particular, were also significantly more abundant in the prenodule and surrounding region compared to the main nodule edge and center. This pattern suggests that these components are expressed and accumulate early in nodule formation, but then as the nodule becomes more mineralized, their expression within the nodule is reduced and they are more involved in the remodeling of the surrounding tissue. Versican and HA, in contrast, were negatively correlated with decorin and biglycan in the prenodule, suggesting that they are less involved in the early nodule formation and more involved in remodeling surrounding the mineralized tissues. Versican and HA may be subjected to paracrine regulation that is distinctive between the prenodules and large mineralized nodules. Another point to consider is that localized stress concentrations may differ between the prenodules and larger nodules, which could stimulate differential PG synthesis and accumulation. Others have also shown differences between nodules of different sizes; for example smaller calcific nodules have more neovascularization than do larger nodules [61]. The HA and versican surrounding the larger nodules might promote improved diffusion of nutrients and oxygen through these thickened valve regions, since diffusion would be enhanced with more highly hydrated tissues. It would be of great interest to examine these speculated mechanisms further in a larger series of calcified valves stratified by clinical characteristics (such as degree of stenosis or identification of bicuspid vs. tricuspid valve), which was unfortunately not possible in this study.

CONCLUSIONS

In conclusion, we have shown that the PGs decorin, biglycan, and versican, and the GAG HA demonstrate distinctive patterns of expression in the vicinity of large and small nodules in calcified aortic valves. The diverse biological and biophysical functions of these extracellular matrix molecules, and the complexities of their regulation, make them compelling subjects for future investigations of the development and treatment of CAVD.

SUMMARY

Proteoglycans decorin, biglycan, and versican, and the glycosaminoglycan hyaluronan were abundant surrounding the calcified nodules from 14 aortic valves, but minimally within the nodule. Decorin and biglycan expression in and surrounding “prenodules” was greater than in the mature nodules. The localization of these matrix components within calcified aortic valves suggests potential roles in lipid retention, cell proliferation, and matrix remodeling.

Acknowledgments

The authors thank the Rice University Institute for Biosciences and Bioengineering Medical Innovations Award for funding. Supported in part by grant HL 63090 (J.D.M.) and a Hertz Foundation Graduate Fellowship (E.H.S.). The authors also thank Kristin Anderson for assistance with the image processing methods.

REFERENCES

1. Stewart BF, Siscovick D, Lind BK, Gardin JM, Gottdiener JS, Smith VE, et al. Clinical factors associated with calcific aortic valve disease. *J Am Coll Cardiol.* 1997; 29:630–634. [PubMed: 9060903]
2. Owens DS, Katz R, Takasu J, Kronmal R, Budoff MJ, O'Brien KD. Incidence and progression of aortic valve calcium in the Multi-Ethnic Study of Atherosclerosis (MESA). *Am J Cardiol.* 2010; 105:701–708. [PubMed: 20185020]
3. Katz R, Wong ND, Kronmal R, Takasu J, Shavelle DM, Probstfield JL, et al. Features of the metabolic syndrome and diabetes mellitus as predictors of aortic valve calcification in the Multi-Ethnic Study of Atherosclerosis. *Circulation.* 2006; 113:2113–2119. [PubMed: 16636166]
4. Schoen FJ. Cardiac valves and valvular pathology: update on function, disease, repair, and replacement. *Cardiovasc Pathol.* 2005; 14:189–194. [PubMed: 16009317]
5. Mohler ER 3rd, Gannon F, Reynolds C, Zimmerman R, Keane MG, Kaplan FS. Bone formation and inflammation in cardiac valves. *Circulation.* 2001; 103:1522–1528. [PubMed: 11257079]
6. Wu B, Elmariah S, Kaplan FS, Cheng G, Mohler ER 3rd. Paradoxical effects of statins on aortic valve myofibroblasts and osteoblasts: implications for end-stage valvular heart disease. *Arterioscler Thromb Vasc Biol.* 2005; 25:592–597. [PubMed: 15618546]
7. Osman L, Yacoub MH, Latif N, Amrani M, Chester AH. Role of human valve interstitial cells in valve calcification and their response to atorvastatin. *Circulation.* 2006; 114:1547–1552. [PubMed: 16820635]
8. Rajamannan NM, Subramaniam M, Stock SR, Stone NJ, Springett M, Ignatiev KI, et al. Atorvastatin inhibits calcification and enhances nitric oxide synthase production in the hypercholesterolaemic aortic valve. *Heart.* 2005; 91:806–810. [PubMed: 15894785]
9. Rajamannan NM, Subramaniam M, Springett M, Sebo TC, Niekrasz M, McConnell JP, et al. Atorvastatin inhibits hypercholesterolemia-induced cellular proliferation and bone matrix production in the rabbit aortic valve. *Circulation.* 2002; 105:2660–2665. [PubMed: 12045173]
10. Caira FC, Stock SR, Gleason TG, McGee EC, Huang J, Bonow RO, et al. Human degenerative valve disease is associated with up-regulation of low-density lipoprotein receptor-related protein 5 receptor-mediated bone formation. *J Am Coll Cardiol.* 2006; 47:1707–1712. [PubMed: 16631011]
11. Moura LM, Ramos SF, Zamorano JL, Barros IM, Azevedo LF, Rocha-Goncalves F, et al. Rosuvastatin affecting aortic valve endothelium to slow the progression of aortic stenosis. *J Am Coll Cardiol.* 2007; 49:554–561. [PubMed: 17276178]
12. Cowell SJ, Newby DE, Prescott RJ, Bloomfield P, Reid J, Northridge DB, et al. A randomized trial of intensive lipid-lowering therapy in calcific aortic stenosis. *N Engl J Med.* 2005; 352:2389–2397. [PubMed: 15944423]
13. Rossebo AB, Pedersen TR, Boman K, Brudi P, Chambers JB, Egstrup K, et al. Intensive lipid lowering with simvastatin and ezetimibe in aortic stenosis. *N Engl J Med.* 2008; 359:1343–1356. [PubMed: 18765433]
14. Miller JD, Chu Y, Brooks RM, Richenbacher WE, Pena-Silva R, Heistad DD. Dysregulation of antioxidant mechanisms contributes to increased oxidative stress in calcific aortic valvular stenosis in humans. *J Am Coll Cardiol.* 2008; 52:843–850. [PubMed: 18755348]
15. O'Brien KD. Pathogenesis of calcific aortic valve disease: a disease process comes of age (and a good deal more). *Arterioscler Thromb Vasc Biol.* 2006; 26:1721–1728. [PubMed: 16709942]
16. Monzack EL, Gu X, Masters KS. Efficacy of simvastatin treatment of valvular interstitial cells varies with the extracellular environment. *Arterioscler Thromb Vasc Biol.* 2009; 29:246–253. [PubMed: 19023089]
17. Sucusky P, Balachandran K, Elhammali A, Jo H, Yoganathan AP. Altered shear stress stimulates upregulation of endothelial VCAM-1 and ICAM-1 in a BMP-4- and TGF-beta1-dependent pathway. *Arterioscler Thromb Vasc Biol.* 2009; 29:254–260. [PubMed: 19023092]
18. Latif N, Sarathchandra P, Taylor PM, Antoniw J, Yacoub MH. Localization and pattern of expression of extracellular matrix components in human heart valves. *J Heart Valve Dis.* 2005; 14:218–227. [PubMed: 15792183]

19. Stephens EH, Chu CK, Grande-Allen KJ. Valve proteoglycan content and glycosaminoglycan fine structure are unique to microstructure, mechanical loads, and age: relevance to an age-specific tissue engineered heart valve. *Acta Biomaterialia*. 2008; 4:1148–1160. [PubMed: 18448399]
20. Reed CC, Iozzo RV. The role of decorin in collagen fibrillogenesis and skin homeostasis. *Glycoconj J*. 2002; 19:249–255. [PubMed: 12975602]
21. Kresse H, Hausser H, Schonherr E, Bittner K. Biosynthesis and interactions of small chondroitin/dermatan sulphate proteoglycans. *Eur J Clin Chem Clin Biochem*. 1994; 32:259–264. [PubMed: 8038266]
22. Nakashima Y, Fujii H, Sumiyoshi S, Wight TN, Sueishi K. Early human atherosclerosis: accumulation of lipid and proteoglycans in intimal thickenings followed by macrophage infiltration. *Arterioscler Thromb Vasc Biol*. 2007; 27:1159–1165. [PubMed: 17303781]
23. Cuff CA, Kothapalli D, Azonobi I, Chun S, Zhang Y, Belkin R, et al. The adhesion receptor CD44 promotes atherosclerosis by mediating inflammatory cell recruitment and vascular cell activation. *J Clin Invest*. 2001; 108:1031–1040. [PubMed: 11581304]
24. Seike M, Ikeda M, Matsumoto M, Hamada R, Takeya M, Kodama H. Hyaluronan forms complexes with low density lipoprotein while also inducing foam cell infiltration in the dermis. *J Dermatol Sci*. 2006; 41:197–204. [PubMed: 16356687]
25. O'Brien KD, Reichenbach DD, Marcovina SM, Kuusisto J, Alpers CE, Otto CM. Apolipoproteins B, (a), and E accumulate in the morphologically early lesion of 'degenerative' valvular aortic stenosis. *Arterioscler Thromb Vasc Biol*. 1996; 16:523–532. [PubMed: 8624774]
26. Chang MY, Potter-Perigo S, Tsoi C, Chait A, Wight TN. Oxidized low density lipoproteins regulate synthesis of monkey aortic smooth muscle cell proteoglycans that have enhanced native low density lipoprotein binding properties. *J Biol Chem*. 2000; 275:4766–4773. [PubMed: 10671509]
27. O'Brien KD, Otto CM, Reichenbach DD, Alpers CE, Wight TN. Regional accumulation of proteoglycans in lesions of "degenerative" valvular aortic stenosis and their relationship to apolipoproteins. *Circulation*. 1995; 92:I-612.
28. Goueffic Y, Potter-Perigo S, Chan CK, Johnson PY, Braun K, Evanko SP, et al. Sirolimus blocks the accumulation of hyaluronan (HA) by arterial smooth muscle cells and reduces monocyte adhesion to the ECM. *Atherosclerosis*. 2007; 195:23–30. [PubMed: 17174314]
29. Itoh S, Matubara M, Kawauchi T, Nakamura H, Yukitake S, Ichinose S, et al. Enhancement of bone ingrowth in a titanium fiber mesh implant by rhBMP-2 and hyaluronic acid. *J Mater Sci Mater Med*. 2001; 12:575–581. [PubMed: 15348249]
30. Kim HD, Valentini RF. Retention and activity of BMP-2 in hyaluronic acid-based scaffolds in vitro. *J Biomed Mater Res*. 2002; 59:573–584. [PubMed: 11774316]
31. Grande-Allen KJ, Calabro A, Gupta V, Wight TN, Hascall VC, Vesely I. Glycosaminoglycans and proteoglycans in normal mitral valve leaflets and chordae: association with regions of tensile and compressive loading. *Glycobiology*. 2004; 14:621–633. [PubMed: 15044391]
32. Grande-Allen KJ, Griffin BP, Calabro A, Ratliff NB, Cosgrove DM III, Vesely I. Myxomatous mitral valve chordae. II: Selective elevation of glycosaminoglycan content. *J Heart Valve Dis*. 2001; 10:325–332. discussion 32-3. [PubMed: 11380095]
33. Grande-Allen KJ, Mako WJ, Calabro A, Shi Y, Ratliff NB, Vesely I. Loss of chondroitin 6-sulfate and hyaluronan from failed porcine bioprosthetic valves. *J Biomed Mater Res*. 2003; 65A:251–259.
34. Grande-Allen KJ, Griffin BP, Ratliff NB, Cosgrove DM, Vesely I. Glycosaminoglycan profiles of myxomatous mitral leaflets and chordae parallel the severity of mechanical alterations. *J Am Coll Cardiol*. 2003; 42:271–277. [PubMed: 12875763]
35. Balachandran K, Konduri S, Sucusky P, Jo H, Yoganathan AP. An ex vivo study of the biological properties of porcine aortic valves in response to circumferential cyclic stretch. *Ann Biomed Eng*. 2006; 34:1655–1665. [PubMed: 17031600]
36. Gupta V, Tseng H, Lawrence BD, Grande-Allen KJ. Effect of cyclic mechanical strain on glycosaminoglycan and proteoglycan synthesis by heart valve cells. *Acta Biomaterialia*. 2009; 5:531–540. [PubMed: 19004676]

37. McCormick D, Chong H, Hobbs C, Datta C, Hall PA. Detection of the Ki-67 antigen in fixed and wax-embedded sections with the monoclonal antibody MIB1. *Histopathology*. 1993; 22:355–360. [PubMed: 8514278]
38. Athanasou NA, Quinn J, Heryet A, Woods CG, McGee JO. Effect of decalcification agents on immunoreactivity of cellular antigens. *J Clin Pathol*. 1987; 40:874–878. [PubMed: 2443541]
39. Ippolito E, LaVelle S, Pedrini V. The effect of various decalcifying agents on cartilage proteoglycans. *Stain Technol*. 1981; 56:367–373. [PubMed: 6803402]
40. Goldberg M, Molon Noblot M, Septier D. [Effect of 2 methods of demineralization on the on the preservation of glycoproteins and proteoglycans in the intertubular and peritubular dentin in the horse]. *J Biol Buccale*. 1980; 8:315–330. [PubMed: 6783643]
41. Fisher LW, Stubbs JT 3rd, Young MF. Antisera and cDNA probes to human and certain animal model bone matrix noncollagenous proteins. *Acta Orthop Scand Suppl*. 1995; 266:61–65. [PubMed: 8553864]
42. Lara SL, Evanko SP, Wight TN. Morphological evaluation of proteoglycans in cells and tissues. *Methods Mol Biol*. 2001; 171:271–290. [PubMed: 11450238]
43. Grande-Allen KJ, Osman N, Ballinger ML, Dadlani H, Marasco S, Little PJ. Glycosaminoglycan synthesis and structure as targets for the prevention of calcific aortic valve disease. *Cardiovasc Res*. 2007; 76:19–28. [PubMed: 17560967]
44. Otto CM, Kuusisto J, Reichenbach DD, Gown AM, O'Brien KD. Characterization of the early lesion of 'degenerative' valvular aortic stenosis. Histological and immunohistochemical studies. *Circulation*. 1994; 90:844–853. [PubMed: 7519131]
45. Camejo G, Hurt-Camejo E, Wiklund O, Bondjers G. Association of apo B lipoproteins with arterial proteoglycans: pathological significance and molecular basis. *Atherosclerosis*. 1998; 139:205–222. [PubMed: 9712326]
46. Ballinger ML, Nigro J, Frontanilla KV, Dart AM, Little PJ. Regulation of glycosaminoglycan structure and atherogenesis. *Cell Mol Life Sci*. 2004; 61:1296–1306. [PubMed: 15170508]
47. Yang BL, Zhang Y, Cao L, Yang BB. Cell adhesion and proliferation mediated through the G1 domain of versican. *J Cell Biochem*. 1999; 72:210–220. [PubMed: 10022503]
48. Matsumoto K, Shionyu M, Go M, Shimizu K, Shinomura T, Kimata K, et al. Distinct interaction of versican/PG-M with hyaluronan and link protein. *J Biol Chem*. 2003; 278:41205–41212. [PubMed: 12888576]
49. Zhang S, Chang MC, Zylka D, Turley S, Harrison R, Turley EA. The hyaluronan receptor RHAMM regulates extracellular-regulated kinase. *J Biol Chem*. 1998; 273:11342–11348. [PubMed: 9556628]
50. Wight TN, Merrilees MJ. Proteoglycans in atherosclerosis and restenosis: key roles for versican. *Circ Res*. 2004; 94:1158–1167. [PubMed: 15142969]
51. Muller B, Prante C, Gastens M, Kuhn J, Kleesiek K, Gotting C. Increased levels of xylosyltransferase I correlate with the mineralization of the extracellular matrix during osteogenic differentiation of mesenchymal stem cells. *Matrix Biol*. 2008; 27:139–149. [PubMed: 17980567]
52. Gupta V, Werdenberg JA, Blevins TL, Grande-Allen KJ. Synthesis of glycosaminoglycans in differently loaded regions of collagen gels seeded with valvular interstitial cells. *Tissue Eng*. 2007; 13:41–49. [PubMed: 17518580]
53. Jian B, Narula N, Li QY, Mohler ER 3rd, Levy RJ. Progression of aortic valve stenosis: TGF-beta1 is present in calcified aortic valve cusps and promotes aortic valve interstitial cell calcification via apoptosis. *Ann Thorac Surg*. 2003; 75:457–465. discussion 65-6. [PubMed: 12607654]
54. Evanko SP, Raines EW, Ross R, Gold LI, Wight TN. Proteoglycan distribution in lesions of atherosclerosis depends on lesion severity, structural characteristics, and the proximity of platelet-derived growth factor and transforming growth factor-beta. *Am J Pathol*. 1998; 152:533–546. [PubMed: 9466580]
55. Kinsella MG, Bressler SL, Wight TN. The regulated synthesis of versican, decorin, and biglycan: extracellular matrix proteoglycans that influence cellular phenotype. *Crit Rev Euk Gene Exp*. 2004; 14:203–234.
56. Allison DD, Grande-Allen KJ. Review. Hyaluronan: a powerful tissue engineering tool. *Tissue Eng*. 2006; 12:2131–2140. [PubMed: 16968154]

57. Evanko SP, Angello JC, Wight TN. Formation of hyaluronan- and versican-rich pericellular matrix is required for proliferation and migration of vascular smooth muscle cells. *Arterioscler Thromb Vasc Biol.* 1999; 19:1004–1013. [PubMed: 10195929]
58. Wilkinson TS, Bressler SL, Evanko SP, Braun KR, Wight TN. Overexpression of hyaluronan synthases alters vascular smooth muscle cell phenotype and promotes monocyte adhesion. *J Cell Physiol.* 2006; 206:378–385. [PubMed: 16110480]
59. Masters KS, Shah DN, Leinwand LA, Anseth KS. Crosslinked hyaluronan scaffolds as a biologically active carrier for valvular interstitial cells. *Biomaterials.* 2005; 26:2517–2525. [PubMed: 15585254]
60. Csoka AB, Frost GI, Stern R. The six hyaluronidase-like genes in the human and mouse genomes. *Matrix Biol.* 2001; 20:499–508. [PubMed: 11731267]
61. Charest A, Pepin A, Shetty R, Cote C, Voisine P, Dagenais F, et al. Distribution of SPARC during neovascularisation of degenerative aortic stenosis. *Heart.* 2006; 92:1844–1849. [PubMed: 16709694]

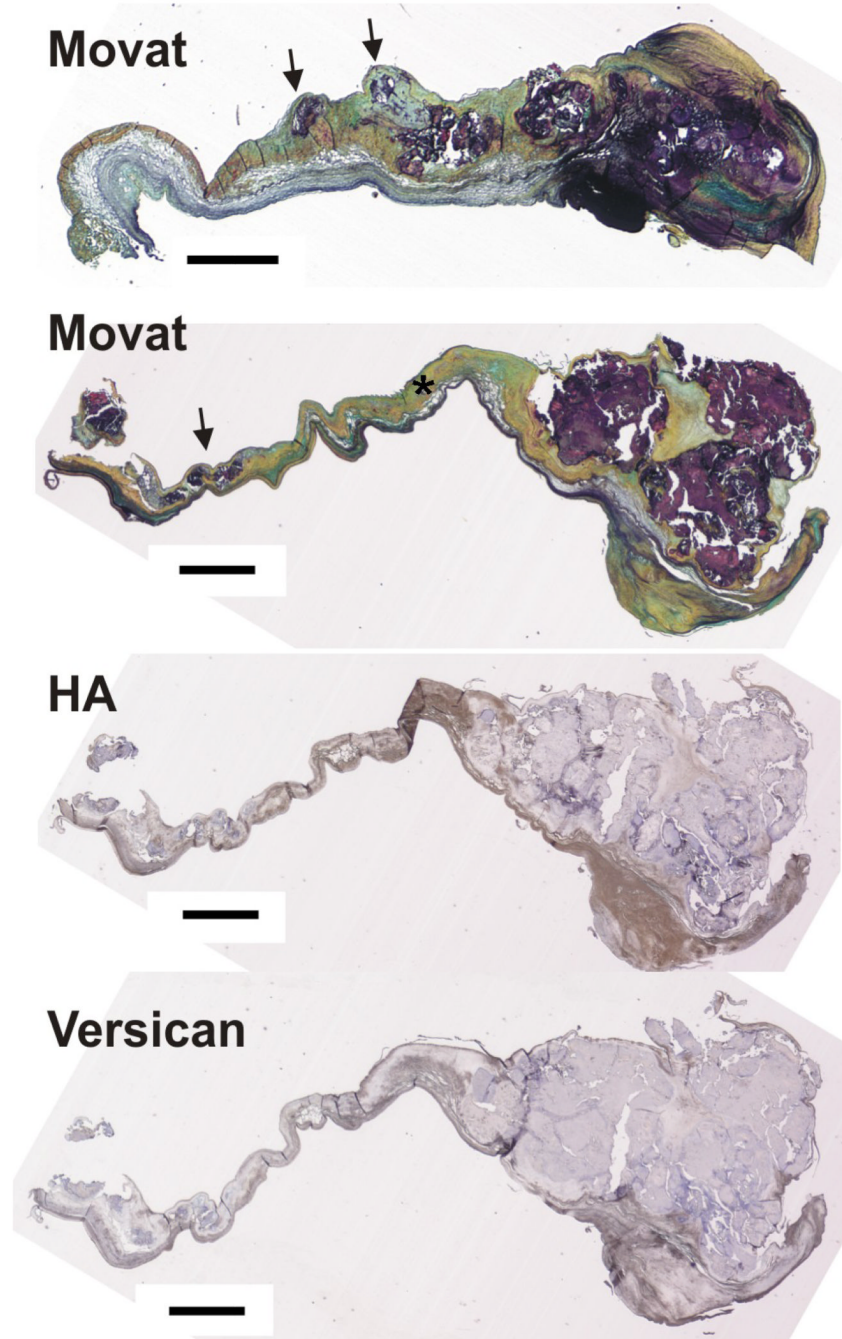
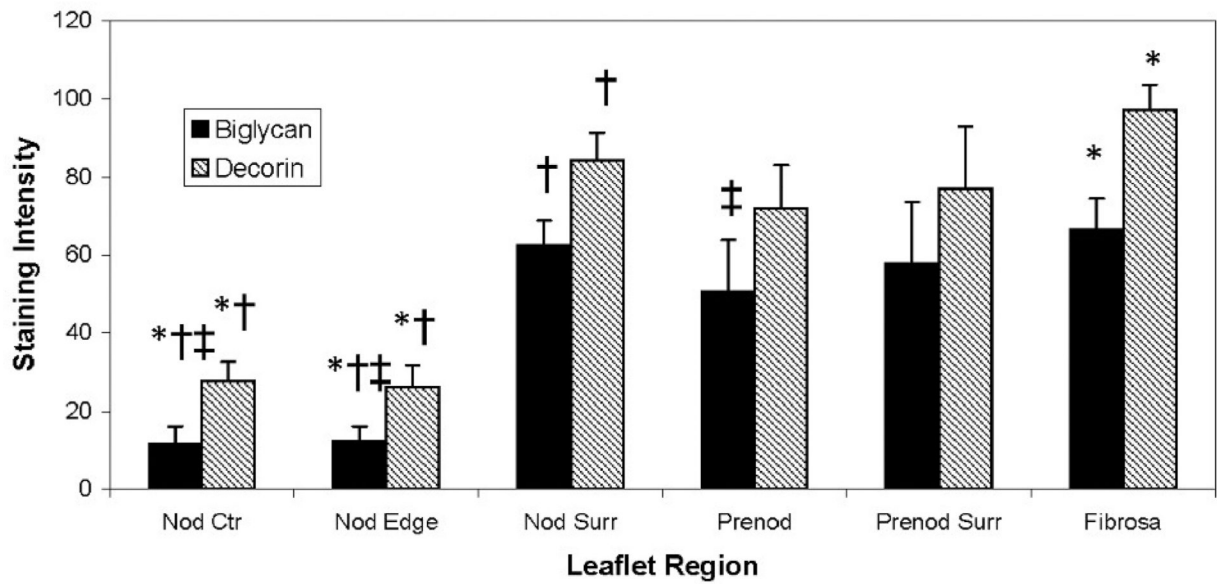


Figure 1.

Upper two images: Movat pentachrome stain of two calcified aortic valves showing large nodules at the distal end and small prenuclei (indicated by arrows) more proximal to the annular edge of the leaflet. Asterisk indicates normal fibrosa. Lower two images: one of the same calcified valves stained for hyaluronan (HA) and versican. Scale bar = 1 mm.

Small Proteoglycan Expression



Versican and Hyaluronan Expression

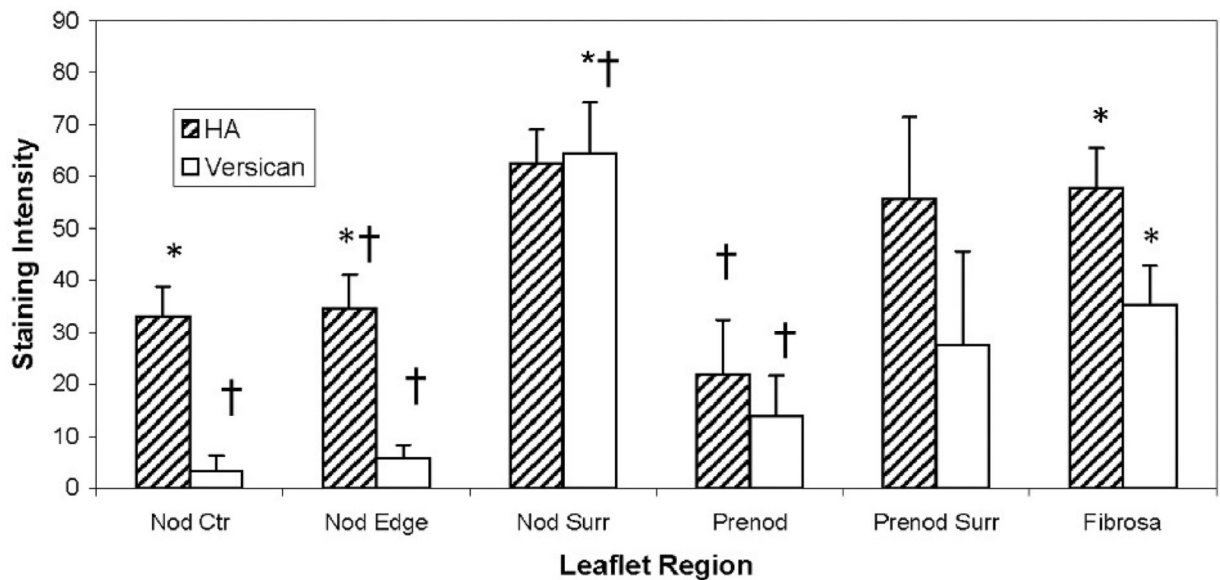


Figure 2.

Intensities of staining for PGs and HA in different regions of calcified aortic valves. Error bars indicate standard error of the mean. † $p < 0.05$ compared to Nod Surr. * $p < 0.05$ compared to Fibrosa. ‡ $p < 0.05$ compared to Prenod. Nod Ctr = innermost 2/3 of the large nodule. Nod Edge = outer 1/3 of the large nodule. Nod Surr = tissue immediately surrounding the large nodule. Prenod = prenodule. Prenod Surr = tissue immediately surrounding the prenodule.

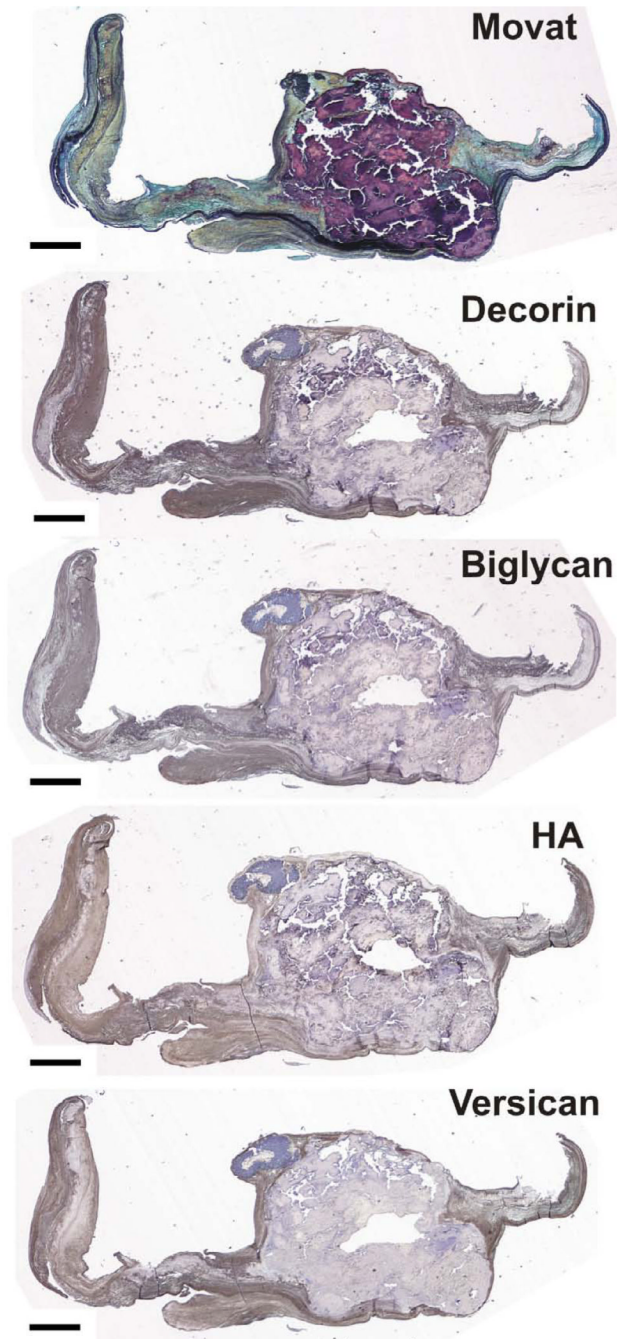


Figure 3. Calcified valve stained with Movat pentachrome and histochemically stained for decorin, biglycan, hyaluronan (HA), and versican. Scale bar = 1 mm.

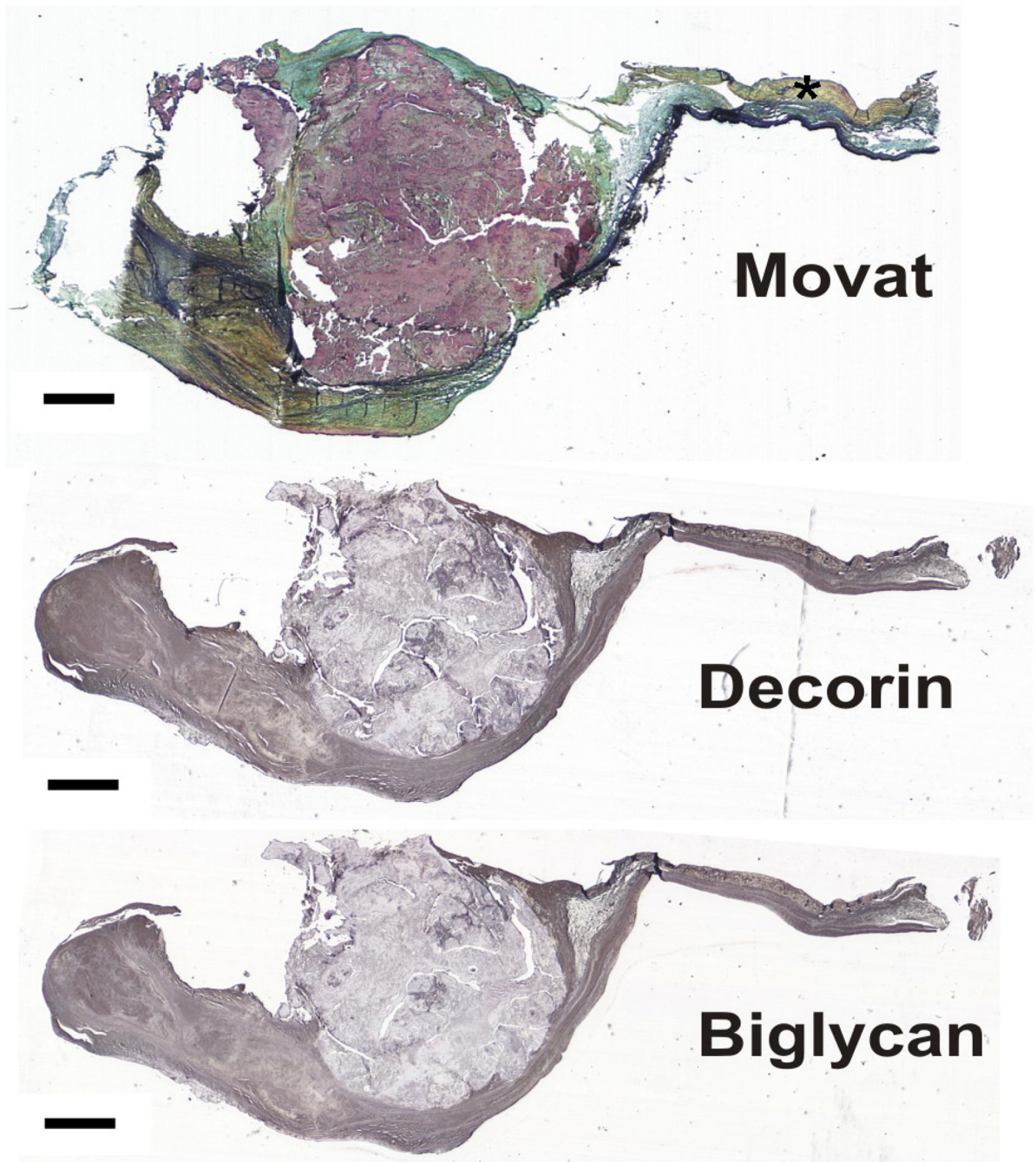


Figure 4. Calcified valve stained with Movat pentachrome and immunohistochemically stained for decorin and biglycan. Asterisk indicates normal fibrosa. Scale bar = 1 mm.